Fluctuation of Motor Charge in the Lateral Membrane of the Cochlear Outer Hair Cell

X.-x. Dong, D. Ehrenstein, and K. H. Iwasa
Biophysics Section, Laboratory of Cellular Biology, National Institute on Deafness and Other Communication Disorders, National Institutes of Health, Bethesda, Maryland 20892-0922 USA

ABSTRACT Functioning of the membrane motor of the outer hair cell is tightly associated with transfer of charge across the membrane. To obtain further insights into the motor mechanism, we examined kinetics of charge transfer across the membrane in two different modes. One is to monitor charge transfer induced by changes in the membrane potential as an excess membrane capacitance. The other is to measure spontaneous flip-flops of charges across the membrane under voltage-clamp conditions as current noise. The noise spectrum of current was inverse Lorentzian, and the capacitance was Lorentzian, as theoretically expected. The characteristic frequency of the capacitance was ~10 kHz, and that for current noise was ~30 kHz. The difference in the characteristic frequencies seems to reflect the difference in the modes of mechanical movement associated with the two physical quantities.

INTRODUCTION

The outer hair cell has a motile mechanism (Brownell et al., 1985) in its lateral membrane that is unique among biological motors in that it is directly dependent on the membrane potential (Ashmore, 1987; Santos-Sacchi and Dilger, 1988). Its motile activity is coupled with transfer of charge across the membrane (Ashmore, 1990; Santos-Sacchi, 1991; Iwasa, 1993). With this mechanism, energy gained by charge transfer is used for mechanical work. Such direct electromechanical coupling, which must be advantageous when operating at high frequencies, was demonstrated by the shift in voltage dependence caused by an increase in membrane tension (Iwasa, 1993; Kakehata and Santos-Sacchi, 1995; Gale and Ashmore, 1995). It is further confirmed by a recent observation that a constraint on the membrane area prevents charge transfer across the membrane (Adachi and Iwasa, 1999). For a further characterization of the motor, we examine here the kinetic properties of charge transfer by the motor.

The easiest method of measuring charge transfer across the membrane is the whole-cell voltage clamp because all motor charges in the cell contribute to the signal, making the signal large. However, this method has a relatively low time resolution, intrinsic to the recording configuration. A low-pass filter is formed by the combination of the access resistance of the recording pipette with the considerable membrane capacitance of the cell. For example, if the membrane capacitance is 20 pF and the recording pipette has an access resistance of 5 MΩ, the circuit has a roll-off frequency lower than 2 kHz for a voltage-clamp experiment. This frequency is significantly lower than the human auditory range, which reaches 20 kHz. The roll-off frequency is lower for a current-clamp experiment because the membrane resistance is usually larger than the access resistance.

The standard on-cell configuration of patch clamp does not have the frequency dependence of the whole-cell mode, but the seal conductance is relatively large for the membrane area recorded. The optimal mode of the recording is expected to be a "giant patch" configuration (Hilgemann, 1995) because it allows recording from larger membrane patches with a seal that is similar to that of the standard on-cell patch technique.

For kinetic study of charge transfer, we measured the frequency dependence of the membrane capacitance and the power spectrum of current noise under voltage clamp, using the giant on-cell patch recording technique. The experimental data are compared with theoretical predictions based on a simple two-state model of the motor (Iwasa, 1997). Preliminary versions of this work have been presented in abstract form (Ehrenstein and Iwasa, 1997).

A SIMPLE TWO-STATE MODEL

Two-state models are successful in describing the motility of the outer hair cell (Ashmore, 1987; Santos-Sacchi and Dilger, 1988; Ashmore, 1990; Santos-Sacchi, 1991; Iwasa, 1993). In these models, two states of the motor differ in their mechanical properties, such as in the membrane area and in the charge distribution across the membrane. Conformational transitions thus involve changes in both charge and mechanical properties of the membrane. Because mechanical changes in the membrane may require mechanical movement, which must follow equations of motion, mechanical constraints and resistance may reciprocally affect transitions of the motor. For the simplest description of motor charge transfer, however, we ignore the reciprocal effect. The following is a brief description of such a theory (Iwasa, 1997). We will be able to examine the possible

Received for publication 10 March 2000 and in final form 14 June 2000.
Address reprint requests to Dr. Kuin H. Iwasa, Biophysics Section, Laboratory of Cellular Biology, National Institute on Deafness and Other Communication Disorders, National Institutes of Health, Building 9, Room 1E120, 9 Center Drive, MSC 0922, Bethesda, MD 20892-0922. Tel.: 301-496-3987; Fax: 301-480-0827; E-mail: kiwasa@helix.nih.gov.

0006-3495/00/10/1876/07 $2.00

effects of electromechanical coupling by comparing the predictions with our experimental data.

Let s and ℓ be two states of a motor unit (with s and ℓ implying small and large membrane area, respectively). The characteristic angular frequency ω_0 ($= 2\pi f_0$) of the system is determined by the sum of the transition rate k_+ from s to ℓ and the rate k_- of the reverse transition. The probability $P_\ell(t)$ that the motor is in state ℓ at time t is given by

$$\frac{dP_\ell(t)}{dt} = -k_- P_\ell(t) + k_+(1 - P_\ell(t)). \quad (1)$$

Equation 1 has a relaxation time $\tau = 1/(k_+ + k_-)$, which corresponds to the characteristic frequency $\omega_0 = 1/\tau$.

The probability P_ℓ that the motor unit is in state ℓ is given by $k_+/(k_+ + k_-)$. The excess membrane capacitance $C_m(\omega)$ and the power spectrum of current noise $S_I(\omega)$ due to the motor are then given, respectively, by (Iwasa, 1997),

$$C_m(\omega) = C_m(0)\frac{\omega_0^2}{\omega^2 + \omega_0^2} \quad (2)$$

$$S_I(\omega) = 4k_B T C_m(0)\frac{\omega_0 \omega^2}{\omega^2 + \omega_0^2} \quad (3)$$

with

$$C_m(0) = \frac{q^2 N}{k_B T}\overline{P_\ell}(1 - \overline{P_\ell}). \quad (4)$$

Here, q is the charge of a motor unit transferable across the membrane, N is the number of motor units in the system, k_B is Boltzmann's constant, and T is the temperature. The quantity $\overline{P_\ell}$ is the equilibrium probability of the motor in the extended conformation, and it is expressed by

$$\overline{P_\ell} = \frac{1}{1 + k_-/k_+} = \frac{1}{1 + \exp[q(V - V_0)/k_B T]}, \quad (5)$$

because the conformational change involves transferring charge q across the voltage difference V. The capacitance has a low-pass (Lorentzian) frequency dependence, and current noise has a high-pass (inverse Lorentzian) frequency dependence.

At the high frequency limit, Eq. 3 is reduced to

$$S_I(\infty) = 4\omega_0 k_B T C_m(0), \quad (6)$$

which will be useful in comparing experimental data on the capacitance and noise.

MATERIALS AND METHODS

Cell preparation

Bullas were obtained from guinea pigs in accordance with the protocol 902-99 NINDS/NIDCD (National Institute of Neurological Disorders and Stroke/ National Institute on Deafness and Other Communication Disorders). The organ of Corti was dissociated from opened cochleas by teasing with a fine needle under a dissection microscope. The strips of organ of Corti thus obtained were triturated three times gently with a plastic pipette and placed in a chamber mounted on an inverted microscope. The lengths of the cells used for the experiment ranged between 40 μm and 75 μm. In some of experiments, dispase (Boehringer-Mannheim) treatment (0.5 units/ml for 20 min at 21°C) was used before mechanical isolation.

Recording setup

We followed the standard method (Hilgemann, 1995) for fabricating giant patch pipettes with a microforge, although the tip diameter was between 2 and 4 μm and was small for pipettes for the giant patch. The pipette resistance was less than 1 MΩ. We found it essential to coat the pipette tips with a mixture of light and heavy mineral oil, following the standard method for the giant patch, to form a tight seal with hair cells.

Giant on-cell patches were formed on the lateral wall of the outer hair cell at locations between the nucleus and the apical end. A channel-blocking medium was used for the bath and in the pipette. The medium contained 100 mM NaCl, 20 mM CsCl, 1.5 mM $MgCl_2$, 20 mM tetraethylammonium, 0.5 M HEPES-Cs, and 2 mM $CoCl_2$. The osmolarity was adjusted to 300 mOs/kg with glucose (~5 mM), and the pH was adjusted to 7.4. The record was taken from cells with a seal resistance that exceeded 2 GΩ.

A stock solution (100 mg/ml) of nystatin (Sigma) was prepared in dimethylsulfoxide. Nystatin was added to the bathing medium and sonicated immediately before use. The final concentration was 0.1 mg/ml.

Data acquisition and analysis

Data acquisition was performed with an Axopatch 200B (Axon Instruments, Foster City, CA) operated in feedback resistor mode in connection with an ITC-16 (Instrutech, Great Neck, NY) driven by the Igor program (WaveMetrics, Lake Oswego, OR), with interface modules created by Bookman Lab at the University of Miami (available from Instrutech at http://www.instrutech.com/archive.html). The voltage dependence of the membrane capacitance was monitored with the phase-tracking technique (Fidler and Fernandez, 1989) at 1 kHz while the DC level was changed stepwise. Circuit modification required for phase tracking in the on-cell configuration was assisted by Axon Instruments. The frequency profile of the capacitance was obtained with fast Fourier transform (FFT) from the current response elicited by a voltage waveform of digitally generated wide-band noise. The noise used had a root mean square amplitude of 5 mV and was 0.325 s in duration. Current noise was recorded in 0.5-s sections. Each data acquisition was repeated at least 20 times. The current output of the patch amplifier was digitized at 10-μs intervals after an 8-pole Bessel filter (model 900; Frequency Devices, Haverhill, MA) operating at 50-kHz corner frequency. The spectra were corrected for the filter in the frequency domain. To improve the signal-to-noise ratio, capacitance compensation was used at the shortest available time constant (10 μs). FFT was performed using 2048 points. The reference records for the pipette capacitance were obtained with the same recording pipette by forming a tight seal on a piece of sylgard located in the same chamber after recording in the cell. As is the case for most on-cell patch experiments, the conductance and the capacitance of the rest of the cell can be ignored in analyzing the record because both are large compared with those of the sealed membrane patch, because of the large difference in the membrane area. The setup was calibrated with a circuit model for on-cell patches before experiments.

RESULTS

Records were taken from giant patches that were formed at the lateral membrane of the outer hair cell. The experiment

was performed in the following sequence. First, the voltage profile of the capacitance was obtained. That was followed by the frequency profile of the membrane capacitance from FFT. Then the current noise spectrum was measured. At the end of the experiment, the pipette used for the experiment was pushed against a piece of sylgard placed on the bottom of the chamber to form a high-resistance seal (~5 GΩ). The frequency profile of the capacitance and the noise spectrum of the sylgard-sealed pipette were used as the baselines.

Voltage dependence of the membrane capacitance

The membrane capacitance consisted of two components. One was the regular membrane capacitance, which was independent of the membrane potential, and the other was nonlinear capacitance, which had a bell-shaped voltage dependence (Fig. 1). The pipette potential of the peak was (55 ± 21) mV (mean ± SD, $N = 46$) and was consistent with the peak membrane potential of ~ −60 mV (Kakehata and Santos-Sacchi, 1995) in the whole-cell recording using channel-blocking media similar to ours. The peak height of the nonlinear capacitance ranged from 30 fF to 300 fF and was typically between 80 fF and 150 fF. The nonlinear component of the capacitance was fitted with Eqs. 3 and 4 to obtain the unit charge q, which determines the steepness, and the number N of such units.

To examine the unit charge obtained with this method, we plotted it against the magnitude of the voltage-dependent component of the membrane capacitance, which may be used as a convenient indicator of the size of the membrane patch (Fig. 2). The plot showed a correlation that larger patches tend to show smaller values for the unit charge q.

During experiments, we usually kept the pipette open to the ambient pressure. In one series of experiments, we

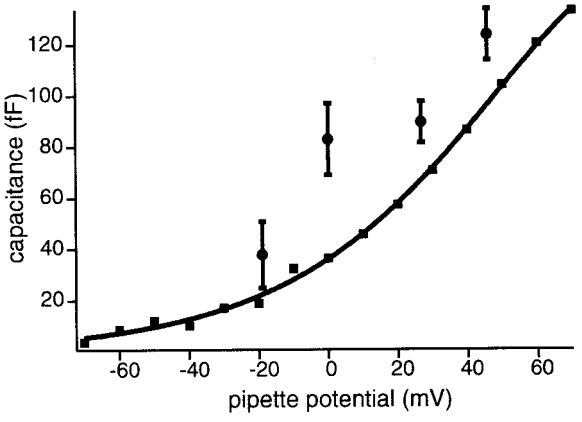

FIGURE 1 The voltage dependence of the membrane capacitance of an on-cell membrane patch formed at the lateral membrane of an outer hair cell. ■: The capacitance obtained with a 1-kHz sinusoidal voltage waveform is plotted against the pipette potential. The baseline is arbitrary. The curve fit (*solid line*) shows that the apparent unit charge q is (0.73 ± 0.06)e (e is the electronic charge), and the number N of motor units is (1.9 ± 0.4) × 10^5: ●, The magnitude of the frequency-dependent component of the capacitance obtained with wideband noise and FFT (see Fig. 3). Error bars indicate standard deviations.

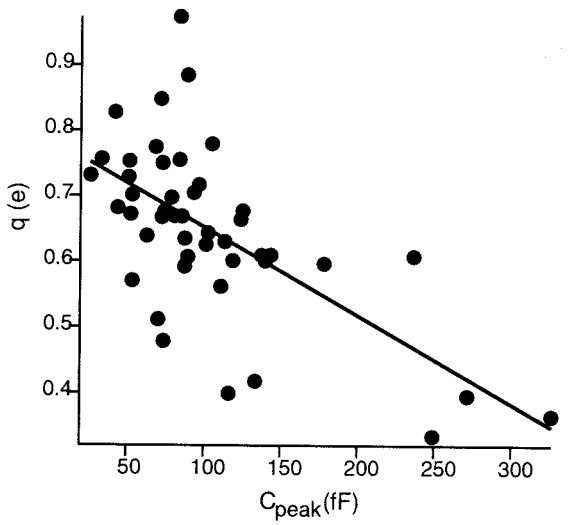

FIGURE 2 The correlation between the apparent unit charge q and the magnitude of the voltage-dependent capacitance. The filled circles represent experimental data and the solid line indicates a best fit (the slope is (−1.34 ± 0.25)e/pF and (0.78 ± 0.03)e at zero capacitance). Pearson's R is 0.63. The magnitude of the voltage-dependent capacitance may be regarded as an indicator of the size of the membrane patch.

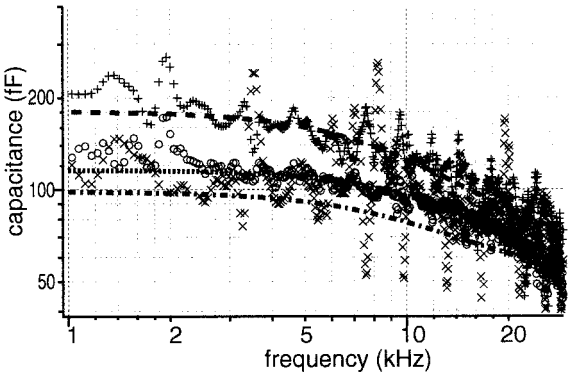

FIGURE 3 The frequency dependence of the membrane capacitance of a membrane patch formed at the lateral membrane of an outer hair cell. This is the patch in Fig. 1. Traces: at pipette potential 45.7 mV (+), 0 mV (○), and −18.9 mV (×). The characteristic frequencies of the three top traces, which are obtained from a curve fit, are, from the top, (12.2 ± 2.0) kHz and (20.7 ± 3.6) kHz. The characteristic frequency of the bottom trace is could not be determined because its value, 7.4 kHz, is about the same as its standard deviation of 6.8 kHz. The values for $C_m(0)$, the magnitude of the frequency-dependent component, are, from the top, (124 ± 10) fF, (83 ± 14) fF, and (38 ± 13) fF, respectively. At pipette potential 26.7 mV (not shown), the characteristic frequency was (12.2 ± 2.2) kHz, and $C_m(0)$ = (90 ± 8) fF. These values are plotted in Fig. 1. The data points plotted are smoothed in the frequency domain to facilitate identification. The curve fit was performed before smoothing.

attempted to determine whether the unit charge q is dependent on pipette pressure. We found that the peak potential was affected by pressure applied to the pipette, but the value for the unit charge q was unaffected by it.

Frequency dependence of the membrane capacitance

The capacitance values near 1 kHz obtained with the FFT method (Fig. 3) were generally consistent with those obtained with phase tracking method. It had a roll-off at around (10.7 ± 4.4) kHz (mean ± SD, $N = 50$).

Hensen's cells were used as a control. Membrane patches formed on those cells had no noticeable voltage dependence of the membrane capacitance. The frequency dependence obtained was also flat (Fig. 4).

In a series of experiments, nystatin (0.1 mg/ml) was added to the bathing medium to determine whether the membrane permeability in the rest of the cell affected our result. Application of nystatin brought about neither a noticeable change in the voltage dependence of the capacitance nor a change in the frequency dependence of the capacitance above 1 kHz.

Power spectrum of current noise

The power spectrum (Fig. 5) of current noise at a given voltage was obtained by subtracting the spectrum of a sylgard patch, which was not voltage dependent, from the giant patch spectrum. The spectrum was high-pass type as expected, with the characteristic frequency usually higher than 30 kHz, exceeding the cutoff frequency of the capacitance spectra (Fig. 5 *A*). The amplitude of noise at a given voltage was well correlated with the capacitance at ~1 kHz. This correlation indicates that the spectrum obtained has a significant contribution from motor charges.

The spectra could be affected by components other than the one due to the motor charge. If the spectra are dominated by fluctuation of the motor charges, subtraction of two spectra obtained at different pipette potentials should have a similar relaxation time.

If these spectra contain a significant contribution from other components, which are not dependent on the membrane potential, the characteristic frequency of the subtraction spectrum may be significantly different from the two individual spectra.

The difference spectra (Fig. 5 *B*) of current noise had a cutoff frequency of about (33.6 ± 9.7) kHz (mean ± SD, $N = 4$). In some membrane patches the frequencies of subtracted spectra were lower than either of the two individual spectra. In those cases the voltage-independent components were larger and had high-pass frequencies higher than 50 kHz. Those observations were consistent with the observation that membrane patches on the Hensen's cells

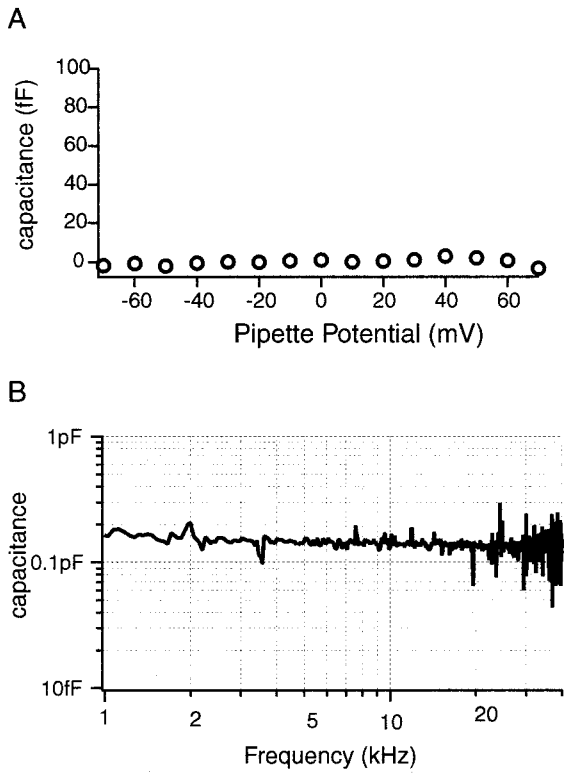

FIGURE 4 The membrane capacitance of a patch formed on a Deiters cell. (*A*) Voltage dependence. (*B*) Frequency dependence.

after sylgard subtraction showed a high-pass current noise spectrum with a characteristic frequency that exceeded 100 kHz.

Because obtaining a seal good enough for the difference noise spectra was extremely difficult, the patches with such records were a small subset of the patches, from which the capacitance was recorded. For those patches with good noise records, the characteristic frequency of the capacitance was (14.3 ± 3.9) kHz (mean ± SD, $N = 4$).

For the power spectrum of noise, the sylgard patch may not always serve as a good control because the effect of the regular (voltage-independent) membrane capacitance remains uncompensated, giving rise to high-pass noise (Benndorf, 1995).

DISCUSSION

Our results have features that are largely consistent with the theoretical predictions based on a simple two-state model, but they do show disagreements in some details. For example, the excess capacitance of tightly sealed giant membrane patches has a bell-shaped peak when plotted against the membrane potential, as predicted by the theory. Nonetheless, the width of the peak shows unpredicted dependence on the size of the membrane patch. The frequency dependence of the membrane capacitance is Lorentzian and the

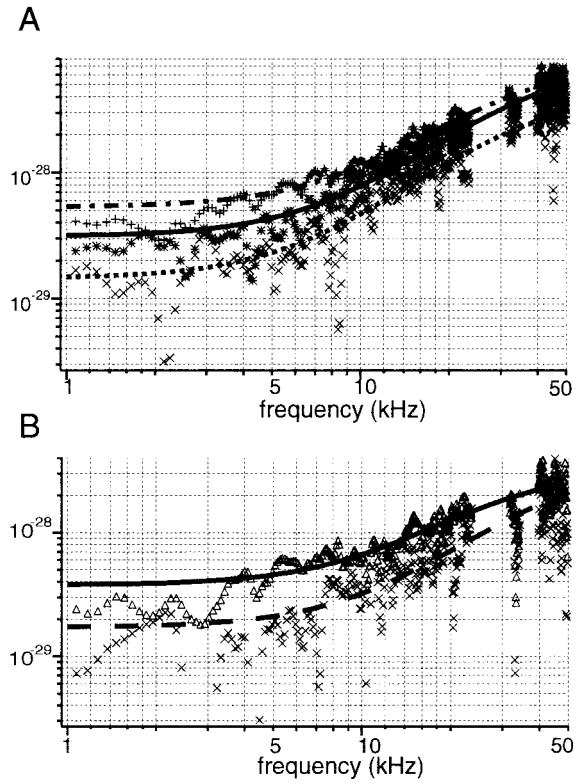

FIGURE 5 The power spectra of current noise. The data points plotted are smoothed in the frequency domain to facilitate identification. The curve fit was performed before smoothing. (*A*) Power spectra of current noise, using the sylgard patch as reference. The data are recorded from the patch shown in Figs. 1 and 3. The characteristic frequency of the inverse Lorentzian is, from the top, (33.0 ± 2.2) kHz for the pipette potential 45.7 mV (+), (39.2 ± 3.6) kHz for 0 mV (*), and (34.8 ± 4.0) kHz for −18.9 mV (×). (*B*) Subtraction spectra of current noise. The spectra are referenced to the spectrum at a pipette potential of −18.9 mV. The relaxation time is (30.4 ± 4.6) kHz at 45.7 mV (△) and (49.8 ± 19.5) kHz at 0 mV (×). The magnitude of the inverse Lorentzian $S_I(\infty)$ is (3.3 ± 0.3) × 10^{-28} A^2s (*top*) and (4.1 ± 1.8) × 10^{-28} A^2s (*bottom*).

power spectrum of membrane current noise is inverse Lorentzian, as predicted. Nonetheless, the characteristic frequency of the capacitance is usually lower than the characteristic frequency of current noise. We will address these discrepancies below.

Motor charge

It has been pointed out previously that the frequency dependence and power spectrum of current noise are not likely to provide additional data for distinguishing a two-state model from a three-state model, beyond what is obtained from the voltage dependence of the membrane capacitance (Iwasa, 1997). We thus discuss motor charge based on a two-state model.

The mean value for the apparent motor charge q_{app} estimated from the voltage dependence of the membrane capacitance in the giant on-cell patches is often ~0.6*e* and is smaller than the value obtained with the whole-cell configuration. The estimate for the motor charge is inversely correlated with the estimated peak height of the nonlinear capacitance, which may be an indicator of the size of the sealed membrane patches (Fig. 2). What is the reason for such a correlation?

The curvature of the membrane patches can be a possible reason. Consider two sealed membrane patches, large and small, which are initially flat. A same hyperpolarizing voltage pulse would makes these membrane patches concave. Membrane tensions T_m in these two patches are equal, and the radius of the curvature r of the larger patch is larger in proportion to the patch diameter. If we assume Laplace's law, $T_m = \frac{1}{2}Pr$, the pressure difference across the membrane is smaller for the smaller patch. Thus movement of the larger patch can be more effectively reduced by other factors in the experimental setup, such as surface tension at the air-water interface in the patch pipette.

An alternative explanation involves interactions between membrane patches and the surface of the glass pipette. It would be plausible that the area of the membrane with such interactions is softer and more flexible than the rest of the membrane, and such an area may extend a fixed distance along the membrane from the seal. Such nonuniformity of the membrane may facilitate area changes when the membrane potential is changed. Because the edge effect is greater in the smaller patch, the motor in the smaller patch is less constrained.

We have attempted to address this issue by applying pressure to the patch pipette because pressure applied to the pipette should affect the curvature of the membrane patch. Pressure application did not have an effect on the apparent value for the motor charge, although it shifted the potential that maximizes the capacitance. This observation favors the explanation by the edge effect.

In either case, the intrinsic motor charge q would then be obtained by extrapolating to the small patch. The extrapolation leads to a value (0.78 ± 0.03)*e*, which is similar to those obtained in the whole-cell configuration (Ashmore, 1990; Santos-Sacchi, 1991; Iwasa, 1993; Kakehata and Santos-Sacchi, 1995).

The characteristic frequency

Our results show that the frequency dependence of the membrane capacitance is low-pass and that the current noise spectrum is high-pass, as theoretically predicted (Eqs. 2 and 3). In addition, the magnitude of noise is larger at the pipette potential, at which the capacitance is larger. However, the characteristic frequencies of the capacitance and that of current noise differ considerably. The expected relationship (Eq. 6) between the capacitance and noise spectrum does not hold because the two characteristic frequencies are not equal.

A basic assumption in the theory that led to the relationship in Eq. 6 is that the charge transfer across the membrane can take place without being affected by any mechanical factor. Can it be a valid assumption in describing a system of motors? In the following we examine this problem.

Effect of viscous resistance

If charge transfer is indeed coupled with motor activity, it would be reciprocally affected by mechanical factors such as resistance and inertia. Transfer of charge across the membrane will not take place until associated mechanical movements occur, which are similar to static constraints (Adachi and Iwasa, 1999).

For microscopic motion, it is likely that viscous resistance would be dominating. The viscous resistance would be proportional to the velocity, which would be related to the rate of transition in motor states. Thus incorporation of such an effect would turn Eq. 1 into

$$\frac{dP_\ell(t)}{dt} = -k_- P_\ell(t) + k_+(1 - P_\ell(t)) - \eta\frac{dP_\ell(t)}{dt}, \quad (7)$$

where the term that involves η represents the effect of friction. Then the relaxation time τ is turned into $(1 + \eta)/(k_+ + k_-)$, leading to the characteristic frequency $\omega_0 = (k_+ + k_-)/(1 + \eta)$.

The viscous drag η could be dependent on the mode of motion. Let η_c represent the drag for collective motion, and let η_s represent the drag for independent motion of a single motor unit. We may then have the characteristic frequency ω_{c0} for collective motion and the frequency ω_{s0} for independent motion, determined by

$$\omega_{c0} = (k_+ + k_-)/(1 + \eta_c). \quad (8)$$

and

$$\omega_{s0} = (k_+ + k_-)/(1 + \eta_s). \quad (9)$$

The relationship (Eq. 6) between the capacitance and the current spectrum should be replaced by

$$S_I(\infty) = 4\omega_{s0}k_B T C_m(0). \quad (10)$$

Another problem we encounter in relating the noise spectrum to the capacitance would be in the value of $C_m(0)$. This is because $C_m(0)$, which is defined by Eq. 4, is proportional to q^2N, and the values q_{app} for the motor charge obtained from our capacitance measurement tend to be smaller than those obtained from other methods as discussed earlier. Because the total motor charge qN tends to be conserved, the difference in $C_m(0)$ would be given by a factor q_{app}/q at the potential that maximizes the capacitance. At potentials away from the peak, the difference is less because a smaller apparent value q_{app} for the charge q makes the voltage dependence of the capacitance less steep. Thus the expected error is up to ~10% if $q_{app} = 0.7e$.

Interpretation of the data

To examine the validity of Eq. 10, we use voltage-dependent differences in the capacitance and current noise. We find that our data approximately satisfy the expected relationship in Eq. 10 (Fig. 6). However, as we have discussed earlier, our capacitance experiment may have underestimated the motor charge due to static constraints. If spontaneous fluctuation of the motor charge is not subjected to such constraints, the observed capacitance values give underestimates of the quantity represented (q^2N) in Eq. 4 of ~10%. This factor actually improves the agreement, although the effect is minor. This agreement suggests that the two modes of our experiments are indeed subjected to different levels of viscous drag. It also provides further evidence for tight electromechanical coupling in the lateral membrane of the outer hair cell.

We deduced that the characteristic frequency for the capacitance experiments is primarily determined by viscous drag in the particular experimental configuration. Our value is similar to the value of 10 kHz reported by Gale and Ashmore (1995), who used sinusoidal voltage waves and obtained their value by pooling data from several standard (smaller) patches.

The characteristic frequency of our data on the current noise spectrum is ~30 kHz. This value could also be affected by viscous drag and could be less than the intrinsic speed of the motor. Thus our data as a whole give 30 kHz as a lower bound for the intrinsic speed of the motor.

There are two reports on the speed of the motor in another recording configuration (Dallos and Evans, 1995; Frank et al., 1999). These reports used the "microchamber" configuration, in which a hair cell is sucked half-way into a

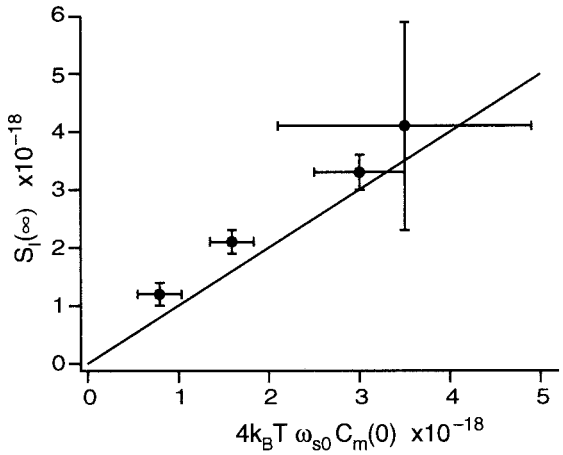

FIGURE 6 The relationship between the capacitance and current noise. The high-frequency asymptote $S_I(\infty)$ of current noise is plotted against the product $4k_BT\omega_{s0}C_m(0)$, where ω_{s0} is the characteristic angular frequency of current noise and $C_m(0)$ is the experimentally determined low-frequency asymptote of the capacitance. The error bars show standard deviations. The solid line represents the prediction of Eq. 10.

suction electrode, partitioning the cell membrane at the pipette tip. Voltage drops take place across the two sides of the cell membrane. With this configuration, cell movement can be elicited by a wide frequency range of voltage waveforms. The roll-off frequency is ~20 kHz or higher (Dallos and Evans, 1995; Frank et al., 1999). Monitoring membrane currents in the "microchamber" configuration is impractical because this configuration cannot be formed with a tight seal between the pipette and the cell membrane.

Force production has also been examined in the "microchamber" configuration, imposing a near-isometric condition. Because no mechanical movement is involved in such a condition, the characteristics of the mechanical elements associated with the motor would be less important. Indeed, the reported characteristic frequency observed under near-isometric condition exceeds 50 kHz (Frank et al., 1999).

The speed of the motor observed in our experiments depends on the recording mode. This dependence appears to reflect the difference in mechanical constraints imposed on the motor in the different modes of our experiments. Our observation can thus be regarded as a manifestation of tight electromechanical coupling in the motor. Our results could also imply that a certain structural support in the lateral wall enables the membrane motor to function at high frequencies. Thus the factor that allows a high-frequency response may not be limited to the molecular structure of the motor alone.

The physiological conditions of the cell are usually closer to current-clamp conditions than to voltage-clamp conditions. Voltage noise associated with motor charge is expected have a similar but more complex frequency dependence (DeFelice, 1981). Motor noise as recorded in the present experiment is not expected to increase the noise level of the membrane potential because high-pass noise with the characteristic frequency of 30 kHz is effectively removed by the circuit characteristics of the cell, which is low-pass with the cutoff frequency up to 1 kHz (Housley and Ashmore, 1992).

CONCLUSIONS

In conclusion, we detected current noise due to flipping of the charge associated with the membrane motor. The observed power spectrum of current noise is high-pass (inverse Lorentzian), and the observed frequency dependence of the capacitance is low-pass (Lorentzian), as expected from a simplified theory in which mechanoelectrical coupling is disregarded. The high-frequency asymptotes of the power spectrum of current noise are well correlated with the low-frequency asymptotes of the capacitance as expected. We found, however, that the characteristic frequency of the current noise spectrum is significantly higher than that of the capacitance, differing from the simplified theory. Such a difference in their characteristic frequencies appears to be the consequence of mechanoelectric coupling, in which the modes of mechanical motion can determine the speed of charge movement.

REFERENCES

Adachi, M., and K. H. Iwasa. 1999. Electrically driven motor in the outer hair cell: effect of a mechanical constraint. *Proc. Natl. Acad. Sci. USA.* 96:7244–7249.

Ashmore, J. F. 1987. A fast motile response in guinea-pig outer hair cells: the molecular basis of the cochlear amplifier. *J. Physiol. (Lond.).* 388: 323–347.

Ashmore, J. F. 1990. Forward and reverse transduction in guinea-pig outer hair cells: the cellular basis of the cochlear amplifier. *Neurosci. Res. Suppl.* 12:S39–S50.

Benndorf, K. 1995. Low-noise recording. *In* Single-Channel Recording. B. Sackmann and E. Neher, editors. Plenum, New York. 129–145.

Brownell, W., C. Bader, D. Bertrand, and Y. Ribaupierre. 1985. Evoked mechanical responses of isolated outer hair cells. *Science.* 227:194–196.

Dallos, P., and B. Evans. 1995. High-frequency motility of outer hair cells and the cochlear amplifier. *Science.* 267:2006–2009.

DeFelice, L. J. 1981. Introduction to Membrane Noise. Plenum, New York.

Ehrenstein, D., and K. H. Iwasa. 1997. Power spectrum of the current noise due to the membrane motor of the cochlear outer hair cell. *Biophys. J.* 72:A236.

Fidler, N., and J. M. Fernandez. 1989. Phase tracking: an improved phase detection technique for cell membrane capacitance measurements. *Biophys. J.* 56:1153–1162.

Frank, G., W. Hemmert, and A. W. Gummer. 1999. Limiting dynamics of high-frequency electromechanical transduction of outer hair cells. *Proc. Natl. Acad. Sci. USA.* 96:4420–4425.

Gale, J., and J. F. Ashmore. 1995. Charge displacement induced by rapid stretch in the basolateral membrane of the guinea-pig outer hair cell. *Proc R. Soc. Lond. (Biol.).* 255:233–249.

Hilgemann, D. W. 1995. The giant membrane patch. *In* Single-Channel Recording. B. Sackmann and E. Neher, editors. Plenum, New York. 307–328.

Housley, G. D., and J. F. Ashmore. 1992. Ionic currents of outer hair cells isolated from the guinea-pig cochlea. *J. Physiol. (Lond.).* 448:73–98.

Iwasa, K. H. 1993. Effect of stress on the membrane capacitance of the auditory outer hair cell. *Biophys. J.* 65:492–498.

Iwasa, K. H. 1997. Current noise spectrum and capacitance due to the membrane motor of the outer hair cell: theory. *Biophys. J.* 73: 2965–2971.

Kakehata, S., and J. Santos-Sacchi. 1995. Membrane tension directly shifts voltage dependence of outer hair cell motility and associated gating charge. *Biophys. J.* 68:2190–2197.

Santos-Sacchi, J. 1991. Reversible inhibition of voltage-dependent outer hair cell motility and capacitance. *J. Neurophysiol.* 11:3096–3110.

Santos-Sacchi, J., and J. P. Dilger. 1988. Whole cell currents and mechanical responses of isolated outer hair cells. *Hear. Res.* 65:143–150.